J|A|C|S
ARTICLES

Published on Web 07/09/2009

Anion-Driven Conformational Polymorphism in Homochiral Helical Coordination Polymers

Guozan Yuan, Chengfeng Zhu, Yan Liu, Weimin Xuan, and Yong Cui*

School of Chemistry and Chemical Technology and State Key Laboratory of Metal Matrix Composites, Shanghai Jiao Tong University, Shanghai 200240, China

Received February 13, 2009; E-mail: yongcui@sjtu.edu.cn

Abstract: Three homochiral 3D frameworks are assembled based on periodically ordered arrays of helices built from axial chiral 3,3′-bipyridine-5,5′,6,6′-tetramethyl-2,2′-dimethoxy-1,1′-biphenyl ligands and linearly coordinated Ag(I) ions. The aggregation behavior of silver salts and the ditopic ligand in solutions was investigated by a variety of techniques, including ^{1}H NMR, UV−vis, CD, GPC and MALDI-TOF. The cationic polymer skeleton exhibits an unprecedented conformational polymorphism in the solid-state, folding into two-, three- and four-fold helices with NO_3^-, PF_6^- and ClO_4^- as the counteranion, respectively. The two-fold helices cross-link *via* argentophilic Ag−Ag interactions to form sextuple helices, which lead to a three-dimensional (3D) chiral framework. The three-fold or four-fold helices, on the other hand, self-associates in pairs to form three-dimensional tubular architectures. This anion-dependent self-assembly behavior can be rationalized by considering the sizes, geometries and binding abilities of the counteranions and subsequent chain conformation to minimize steric repulsions and maximize secondary interactions.

Introduction

Helical and homochiral structures are ubiquitous in nature and are integral to various biological functions.[1] Natural biopolymers such as DNA and proteins have acquired a definite helical sense (e.g., right handed α-helix) associated with the homochirality of their components (e.g., D-sugars and L-amino acids).[2] Conformational polymorphism of helical architectures is a commonly observed phenomenon in biopolymers and is of significant interest because polymorphs can lead to different physicochemical properties and functions, but the decisive physical principles governing conformational polymorphism remain poorly understood.[3]

Chemists have made great efforts to introduce helicity into artificial systems.[4] In particularly, the study of supramolecular helical polymers that have the potential to undergo conformational changes triggered by external stimuli, structurally comparable to those of natural biopolymers, is of significant importance not only in gaining new insight on the parameters that influence the foldability of a backbone but also in preprogramming molecules to give specific architecture and defined functionality.[5−8] With a few notable exceptions, however, the synthetic polymers fold into one or two helical conformations, and no multiple conformational polymorphism has been observed for helical coordination polymers.[7−9]

Coordination polymers based on monomer units that are held together by coordinative bonds are currently attracting extensive interest due to their potential applications in catalysis, sensor, photonics and electronics.[10] The modular nature of coordination polymers means they are readily tunable, and as a result, a careful selection of appropriate ligands and metals may lead to

(1) (a) Bonner, W. A. *Top. Stereochem.* **1988**, *18*, 1–96. (b) Bada, J. L. *Nature* **1995**, *374*, 594–595.
(2) (a) Goodman, G.; Gershwin, M. E. *Exp. Biol. Med.* **2006**, *231*, 1587–1592. (b) Bonner, W. A. *Biosphere* **1994**, *24*, 63 Origins Life Evol.
(3) (a) Satheeshkumar, K. S.; Jayakumar, R. *Biophys. J.* **2003**, *85*, 473–483. (b) Degioia, L.; Selvaggini, C.; Ghibaudi, E.; Diomede, L.; Bugiani, O.; Forloni, G.; Tagliavini, F.; Salmona, M. *J. Biol. Chem.* **1994**, *269*, 7859–7862. (c) Reich, Z.; Ghirlando, R.; Minsky, A. *Biochemistry* **1991**, *30*, 7828–7836.
(4) (a) Nakano, T.; Okamoto, Y. *Chem. Rev.* **2001**, *101*, 4013–4038. (b) Cornelissen, J. J. L. M.; Rowan, A. E.; Nolte, R. J. M.; Sommerdijk, N. A. J. M. *Chem. Rev.* **2001**, *101*, 4039–4070. (c) Albrecht, M. *Chem. Rev.* **2001**, *101*, 3457–3497. (d) Brunsveld, L.; Folmer, B. J. B.; Meijer, E. W.; Sijbesma, R. P. *Chem. Rev.* **2001**, *101*, 4071–4098. (e) Volker Berl, V.; Huc, I.; Khoury, R. G.; Krische, M. J.; Lehn, J.-M. *Nature* **2000**, *407*, 720–723. (f) Gellman, S. H. *Acc. Chem. Res.* **1998**, *31*, 173.
(5) (a) Stone, M. T.; Moore, J. S. *J. Am. Chem. Soc.* **2005**, *127*, 5928–5935. (b) Nelson, J. C.; Saven, J. G.; Moore, J. S.; Wolynes, P. G. *Science* **1997**, *277*, 1793–1796. (c) Prince, R. B.; Okada, T.; Moore, J. S. *Angew. Chem., Int. Ed.* **1999**, *38*, 233–236. (d) Gin, M. S.; Yokozawa, T.; Prince, R. B.; Moore, J. S. *J. Am. Chem. Soc.* **1999**, *121*, 2643–2644. (e) Hill, D. J.; Mio, M. J.; Prince, R. B.; Hughes, T. S.; Moore, J. S. *Chem. Rev.* **2001**, *101*, 3893–4012.
(6) (a) Kim, H.-J.; Lee, E.; Park, H.; Lee, M. *J. Am. Chem. Soc.* **2007**, *129*, 10994–10995. (b) Barboiu, M.; Lehn, J.-M. *Proc. Natl. Acad. Sci. U.S.A.* **2002**, *99*, 5201–5206. (c) Pengo, P.; Pasquato, L.; Moro, S.; Brigo, A.; Fogolari, F.; Broxterman, Q. B.; Kaptein, B.; Scrimin, P. *Angew. Chem., Int. Ed.* **2003**, *42*, 3388–3392.
(7) (a) Yashima, E.; Maeda, K.; Yoshio, F. *Acc. Chem. Res.* **2008**, *41*, 1166–1180. (b) Kim, H.; Lim, Y.; Lee, M. *J. Polym. Sci., Part A: Polym. Chem.* **2008**, 1925–1935.
(8) (a) Chen, X.-D.; Du, M.; Mak, T. C. W. *Chem. Commun.* **2005**, 4417–4419. (b) Jung, O.-S.; Kim, Y. J.; Lee, Y.-A.; Park, J. K.; Chae, H. K. *J. Am. Chem. Soc.* **2000**, *123*, 9921–9925. (c) Robin, A. Y.; Fromm, K. M. *Coord. Chem. Rev.* **2006**, *250*, 2127–2157.
(9) (a) Cui, Y.; Lee, S. J.; Lin, W. *J. Am. Chem. Soc.* **2003**, *125*, 6014–6015. (b) Tabellion, F. M.; Seidel, S. R.; Arif, A. M.; Stang, P. J. *Angew. Chem., Int. Ed.* **2001**, *40*, 1529–1532. (c) Biradha, K.; Seward, C.; Zaworotko, M. J. *Angew. Chem., Int. Ed.* **1999**, *38*, 492–495. (d) Kimura, M.; Sano, M.; Muto, T.; Hanabusa, K.; Shirai, H. *Macromolecules* **1999**, *32*, 7951–7953.
(10) (a) Yaghi, O. M.; O'Keeffe, M.; Ockwig, N. W.; Chae, H. K.; Eddaoudi, M.; Kim, J. *Nature* **2003**, *423*, 705–714. (b) Moulton, B.; Zaworotko, M. J. *Chem. Rev.* **2001**, *101*, 1629–1658.

10.1021/ja901154p CCC: $40.75

coordination polymers with desirable structure and functionality based on their coordination tendencies and geometries. In this context, the synthesis of homochiral helical polymers exhibiting multiple conformations can be envisioned by a judicious choice of two-coordinate metal nods and twisted bridging ligands.[8−10]

In this study, we have synthesized a C_2-symmetric twisted bispyridyl-based biphenyl ligand to form chiral helical Ag(I) coordination polymers and characterized the resulting polymers by NMR, UV−vis, circular dichroism (CD), gel permeation chromatography (GPC) measurement, and powder and single-crystal X-ray diffraction. The cationic polymer skeleton exhibits an unprecedented conformational polymorphism and adjusts its conformation to fold into 2_1, 3_1 and 4_1 helices in response to the counteranions NO_3^-, PF_6^- and ClO_4^-, respectively. Note that 1,1′-biphenyl derivatives bearing intrinsic C_2 symmetry constitute a class of compounds widely employed in chiral recognition and asymmetric synthesis. The ability to incorporate such chiral auxiliaries into helical backbones, which is exploitable for enantioselective processes, represents a major step toward the development of functional supramolecular systems.[11,12]

Experimental Methods

General. All of the chemicals are commercial available, and used without further purification. Elemental analyses were performed with an EA1110 CHNS-0 CE elemental analyzer. The IR (KBr pellet) spectrum was recorded (400−4000 cm^{-1} region) on a Nicolet Magna 750 FT-IR spectrometer. The CD spectra were recorded on a J-800 spectropolarimeter (Jasco, Japan). Thermogravimetric analyses (TGA) were carried out in an N_2 atmosphere with a heating rate of 10 °C/min on a STA449C integration thermal analyzer. Powder X-ray diffraction (PXRD) data were collected on a DMAX2500 diffractometer using Cu Kα radiation. The calculated PXRD patterns were produced using the SHELXTL-XPOW program and single crystal reflection data. All fluorescence measurements were carried out on a LS 50B Luminescence Spectrometer (Perkin-Elmer, Inc., USA). All UV/vis absorption spectrum were recorded on a Lambda 20 UV/vis Spectrometer-(Perkin-Elmer, Inc., USA). ^1H and ^{13}C NMR experiments were carried out on a MERCURYplus 400 spectrometer operating at resonance frequencies of 100.63 MHz. Mass spectra (ESI and MALDI-TOF) were obtained on a Finnigan LCQ mass or Voyager-DE STR spectrometer. Molecular weights were measured with a Water GPC system using polystyrene as the standard and DMF as the eluent.

Synthesis of (*R*)-3,3′-Dibromo-5,5′,6,6′-tetramethyl-2,2′-diol-1,1′-biphenyl. To a solution of (*R*)-5,5′,6,6′-tetramethyl-2,2′-diol-1,1′-biphenyl (3.47 g, 14.3 mmol) in 100 mL $CHCl_3$, Br_2 (1.7 mL, 32.2 mmol) in 20 mL $CHCl_3$ was added dropwise over 20 min. The mixture was stirred at room temperature for 1 h. The reaction was quenched by addition of saturated Na_2SO_3. The aqueous layer was extracted with Et_2O (3 × 20 mL), the combined organic layers were washed with water and brine, and dried over Na_2SO_4. The solution was concentrated under reduced pressure to afford (*R*)-3,3′-dibromo-5,5′,6,6′-tetramethyl-1,1′-biphenyl-2,2′-diol as an off-white solid (5.61 g, 98.0%). ^1H NMR (400 MHz, $CDCl_3$) δ: 1.86 (s, 6H), 2.25(s, 6H), 5.12(s, 2H), 7.35 (s, 2H).

Synthesis of (*R*)-3,3′-Dibromo-5,5′,6,6′-tetramethyl-2,2′-dimethoxy-1,1′-biphenyl. To a mixture of (*R*)-3,3′-dibromo-5,5′,6,6′-tetramethyl-1,1′-biphenyl-2,2′-diol (7.4 g, 18.5 mmol), K_2CO_3 (8.6 g, 62.3 mmol) in 80 mL acetone, MeI (10.4 g, 73 mmol) was added all at once. The mixture was stirred at room temperature overnight. The organic layer was separated and the aqueous layer was extracted with CH_2Cl_2 (3 × 50 mL). The combined organic layers were washed with brine, dried over Na_2SO_4 and filtered. The solution was concentrated under reduced pressure to afford (*R*)-3,3′-dibromo-5,5′,6,6′-tetramethyl-2,2′-dimethoxy-1,1′-biphenyl as a white solid (7.74 g, 98.0%). ^1H NMR (400 MHz, $CDCl_3$) δ: 1.84 (s, 6H), 2.26 (s, 6H), 3.50 (s, 6H), 7.39 (s, 2H).

Synthesis of (*R*)-3,3′-Bipyridine-5,5′,6,6′-tetramethyl-2,2′-dimethoxy-1,1′-biphenyl (L). (*R*)-3,3′-Dibromo-5,5′,6,6′-tetramethyl-2,2′-dimethoxy-1,1′-biphenyl (6.0 g, 14.1 mmol), 4-pyridylboronic acid (3.46 g, 28.2 mmol), Na_2CO_3 (7.46 g, 70.4 mmol) and $PdCl_2(dppf)\cdot CH_2Cl_2$ (0.58 g, 0.7 mmol) were weighted into a 150 mL Schlenk flask which was then pump-purged with N_2 three times. DME(60 mL) and H_2O (30 mL) were added under a dry N_2 atmosphere. The mixture was heated to reflux with stirring and maintained at this temperature for 24 h. The reaction mixture was cooled to room temperature and extracted with CH_2Cl_2. The combined organic layers were washed several times with brine, dried over $MgSO_4$ and then concentrated under reduced pressure. The crude product was purified by column chromatography on silica gel (2:1 hexane-EtOAc) to afford (*R*)-5,5′,6,6′-tetramethyl-2,2′-dimethoxy-1,1-biphenyl-3,3′-bipyridines **L** as a white solid (5.73 g, 96.0%). ^1H NMR (400 MHz, $CDCl_3$) δ: 1.98 (s, 6H), 2.34 (s, 6H), 3.19 (s, 6H), 7.21(s, 2H), 7.56(d, J = 5.6 Hz, 4H), 8.62(d, J = 5.6 Hz, 4H); ^{13}C NMR ($CDCl_3$, 400 MHz) δ: 17.18, 20.38, 60.70, 123.98, 128.97, 131.12, 132.51, 132.98, 137.59, 147.14, 150.00, 153.72; MS (ESI) *m*/*z*: 425.3 ($M^+ + 1$), 426.3 ($M^+ + 2$). The ligand (*S*)-**L** was synthesized similarly.

Synthesis of Compounds 1−3. A mixture of AgX (0.05 mmol; X = ClO_4^-, PF_6^- or NO_3^-), the ligand **L** (0.05 mmol), H_2O (1 mL), MeOH (or *i*-PrOH) (2 mL) and CH_3CN (1 mL) was stirred for 10 min to give a clear solution and then it was allowed to stand at room temperature. After four days, colorless blocklike crystals of **1**−**3** suitable for single-crystal X-ray diffraction were collected, washed with ether and dried in air. The products were not significantly affected by a change in the molar ratio of Ag(I) and **L** (1:1, 2:1 or 1:2). Moreover, when ethanol was used as a solvent instead of methanol or isopropanol, the same crystalline products were obtained.

The products can be best formulated as [Ag**L**(NO_3)], [Ag**L**-$(PF_6)_{1/6}(OH)_{5/6}$] and [Ag**L**(ClO_4)] for **1**−**3**, respectively, on the basis of microanalysis, IR and TGA. While the single-crystal diffraction showed that the products have the formula [(Ag**L**)NO_3]·*i*-PrOH·8/3H_2O (**1**), [Ag(**L**)$(PF_6)_{1/6}(OH)_{5/6}$]·3/2MeOH·CH_3CN·3/2H_2O (**2**) and [Ag(**L**)ClO_4]·3H_2O (**3**). This difference may be attributed to the fact that the products readily lose the guest molecules upon exposure to air. Yield: **1**, 23.7 mg, 80%; **2**, 18.8 mg, 81%; **3**, 24.6 mg, 78%.

Elemental Analysis data and IR of **1**: Anal. (%). Calcd for [Ag**L**(NO_3)] $C_{28}H_{28}AgN_3O_5$: C, 56.58; H, 4.75; N, 7.07. Found: C, 55.97; H, 4.70; N, 7.00. FTIR (KBr pellet): 3445.70(m), 2935.12(m), 2364.83(w), 1608.30(s), 1540.29(w), 1463.79(m), 1384.46(s), 1322.73(s), 1299.03(s), 1218.31(s), 1049.30(s), 957.98(w), 836.10(m), 777.15(w), 701.81(w), 652.65(w).

Elemental Analysis data and IR of **2**: Anal. (%). Calcd for [Ag**L**$(PF_6)_{1/6}(OH)_{5/6}$] $C_{28}H_{28.83}AgF_{1.02}N_2O_{2.83}P_{0.17}$: C, 58.88; H, 5.09; F, 3.39; N, 4.90. Found: C, 57.93; H, 5.02; F, 3.32; N, 4.88. FTIR (KBr pellet): 3489.90(s), 2932.50(s), 2461.53(w), 1606.81(s), 1539.72(m), 1506.05(w), 1456.22(m), 1423.89(s), 1388.49(s), 1325.55(w), 1222.29(m), 1059.26(s), 835.20(m), 721.57(m), 568.06(w)

Elemental Analysis data and IR of **3**: Anal. (%). Calcd for [Ag**L**(ClO_4)] $C_{28}H_{28}AgClN_2O_6$: C, 53.22; H, 4.47; Cl, 5.61; N, 4.43. Found: C, 52.91; H, 4.42; Cl, 5.52; N, 4.39. FTIR (KBr pellet): 3446.11(s), 2936.26(m), 2364.83(w), 1610.00(s), 1458.63(s), 1423.17(s), 1300.82(w), 1222.56(m), 958.90(w), 835.49(m), 702.46(w), 621.93(m), 568.76(w).

(11) (a) Seo, J. S.; Whang, D.; Lee, H.; Jun, S. L.; Oh, J.; Jeon, Y. J.; Kim, K. *Nature* **2000**, *404*, 982–986. (b) Wu, C.-D.; Hu, A.; Zhang, L.; Lin, W. *J. Am. Chem. Soc.* **2005**, *127*, 8940–8941. (c) Li, G.; Yu, W.; Cui, Y. *J. Am. Chem. Soc.* **2008**, *130*, 4582–4583.

(12) (a) Hua, Z.; Vassar, V. C.; Ojima, I. *Org. Lett.* **2003**, *5*, 3831–3834. (b) Sattely, E. S.; Cortez, G. A.; Moebius, D. C.; Schrock, R. R.; Hoveyda, A. H. *J. Am. Chem. Soc.* **2005**, *127*, 8526–8533.

Table 1. Crystal Data and Structure Refinement for Complexes **1**−**3**

	1	2	3
formula	$C_{93}H_{124}Ag_3N_9O_{26}$	$C_{31.50}H_{40.83}AgFN_3O_{5.83}P_{0.17}$	$C_{28}H_{34}AgClN_2O_9$
morphology	block	block	block
color	colorless	colorless	colorless
crystal size (mm^3)	0.22 × 0.18 × 0.16	0.16 × 0.15 × 0.14	0.22 × 0.16 × 0.12
crystal system	tetragonal	trigonal	tetragonal
space group	$P4_12_12$	$R32$	$P4_322$
unit cell dimensions			
$a = b$ (Å)	28.7749(3)	23.6519(3)	17.4625(2)
c (Å)	24.4911(6)	39.4914(10)	24.1023(7)
$\alpha = \beta$ (deg)	90	90	90
γ (deg)	90	120	90
volume (Å^3)	20278.5(6)	19132.2(6)	7349.7(2)
T (K)	123(2)	123(2)	123(2)
wavelength (Å)	1.54178	1.54178	1.54178
reflns measured	44201	16621	15598
data /restraint/parameters	10574/19/917	5783/8/406	3734/26/324
independent reflns	10547	5783	3734
R(int)	0.0373	0.0337	0.0390
Final R indices	R1 = 0.0640,	R1 = 0.0521,	R1 = 0.0598,
[$I > 2\sigma$ (I)]	wR2 = 0.1693	wR2 = 0.1502	wR2 = 0.1588
R indices (all data, F^2 refinement)	R1 = 0.0665,	R1 = 0.0542,	R1 = 0.0602,
	wR2 = 0.1718	wR2 = 0.1535	wR2 = 0.1592
GOF on F^2	1.039	1.093	1.064
flack parameter	0.020(9)	−0.005(10)	0.042(17)

UV−Vis and CD Spectroscopic Measurements. UV−vis absorption spectra were recorded using on a Lambda 20 UV/vis Spectrometer(Perkin-Elmer, Inc., USA). A 100 mL amount of a 25 μM solution of (*S*)-**L** in methanol was titrated with an AgX solution ($AgNO_3$, 3.4 mg/ 10 mL, H_2O, 2 mM; $AgPF_6$, 5.1 mg/ 10 mL, methanol, 2 mM; $AgClO_4$, 4.1 mg/ 10 mL, methanol, 2 mM.), and the UV−vis spectra were measured in a 1 cm quartz cell. Circular dichroism spectra (CD) were recorded in 1 mm quartz cells at 20 °C on a J-800 spectropolarimeter (Jasco, Japan). In a typical titration experiment, a 100 mL amount of a 0.5 mM solution of (*S*)-**L** in methanol was titrated with an AgX solution ($AgNO_3$, 68.0 mg/ 10 mL, H_2O, 40 mM; $AgPF_6$, 102.0 mg/ 10 mL, methanol, 40 mM; $AgClO_4$, 82.0 mg/ 10 mL, methanol, 40 mM), the CD spectra were taken every time after 2 min of vigorous mixing.

Single-Crystal X-ray Diffraction. Single-crystal XRD data for compounds **1**−**3** were all collected on a Bruker SMART Apex II CCD-based X-ray diffractometer with Cu Kα radiation (λ = 1.54178 Å) at 123 K. The empirical absorption correction was applied by using the SADABS program (G. M. Sheldrick, SADABS, program for empirical absorption correction of area detector data; University of Göttingen, Göttingen, Germany, 1996). The structure was solved using direct method, and refined by full-matrix least-squares on F^2 (G. M. Sheldrick, SHELXTL97, program for crystal structure refinement, University of Göttingen, Germany, 1997). In all compounds, the guest molecules and H-atoms were refined isotropically, while all other atoms were refined anisotropically. Crystal data and details of the data collection are given in Tables 1 and S1, Supporting Information, while selected bond distances and angles are presented in Tables S2−4, Supporting Information.

Results and Discussion

Synthesis. The enantiopure atropisomeric ligand **L** was synthesized in 96% yield by Suzuki coupling reaction between 4-pyridylboronic acid and 3,3′-dibromo-2,2′-dimethoxy-5,5′,6,6′-tetramethyl-1,1′-biphenyl, which was obtained in two steps in excellent overall yield from 5,5′,6,6′-tetramethyl-2,2′-diol-1,1′-biphenyl (Scheme 1). The **L** ligand was fully characterized by ^{1}H and ^{13}C NMR, ESI-MS, UV−vis, and CD spectra.

Single crystals of [(Ag**L**)NO_3] (**1**), [Ag(**L**)$(PF_6)_{1/6}(OH)_{5/6}$] (**2**) and [Ag(**L**)ClO_4] (**3**) were readily obtained in good yields by slow evaporation of a solution of the corresponding silver(I) salts and **L** in a mixture of water, methanol (or isopropanol) and acetonitrile. The formulations were supported by microanalysis, IR, and thermogravimetric analysis (TGA) and single-crystal X-ray diffraction. The reaction was originally accomplished in a 1:1 molar ratio of Ag(I) and **L**, but the products were not significantly affected by a change of the molar ratio. Moreover, when ethanol was used as a solvent instead of methanol and isopropanol, the same products were obtained. The products **1**−**3** are thus favorable species irrespective of the reactant molar ratios and concentrations and the organic solvents used. The phase purity for the bulk samples of **1**−**3** has been established by comparison of their observed and simulated X-ray powder diffraction patterns (Figure S19 in the Supporting Information).

Scheme 1. Synthesis of the Ligand **L** and Helical Polymers **1**−**3**

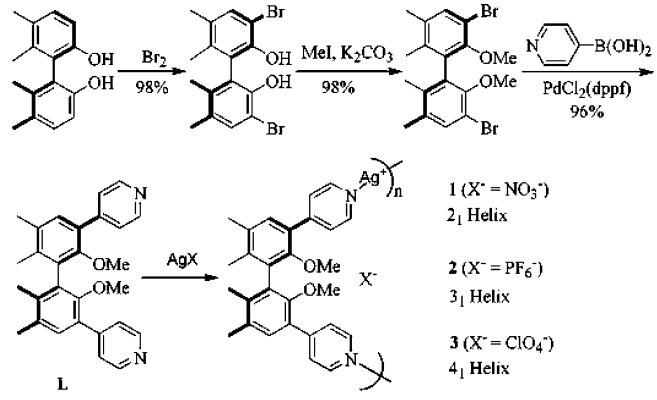

The Self-Assembly Behavior of Ag(I) and L. The self-assembly behavior of silver salts and **L** in solutions was first investigated by ^{1}H NMR spectroscopy. Upon mixing equimolar amounts of **L** and AgX in d^4-MeOH/D_2O (X = NO_3^-) or d^4-MeOH (X = ClO_4^- or PF_6^-), the ^{1}H NMR spectra of the reaction mixtures each exhibit well-resolved signals for a single ligand environment. The C_2-symmetry of the biphenyl ligand **L** is preserved in each cases, as could be deduced from the number of signals in the ^{1}H NMR spectra. With the passage of time, the resonances first gradually broaden to reach a maximum

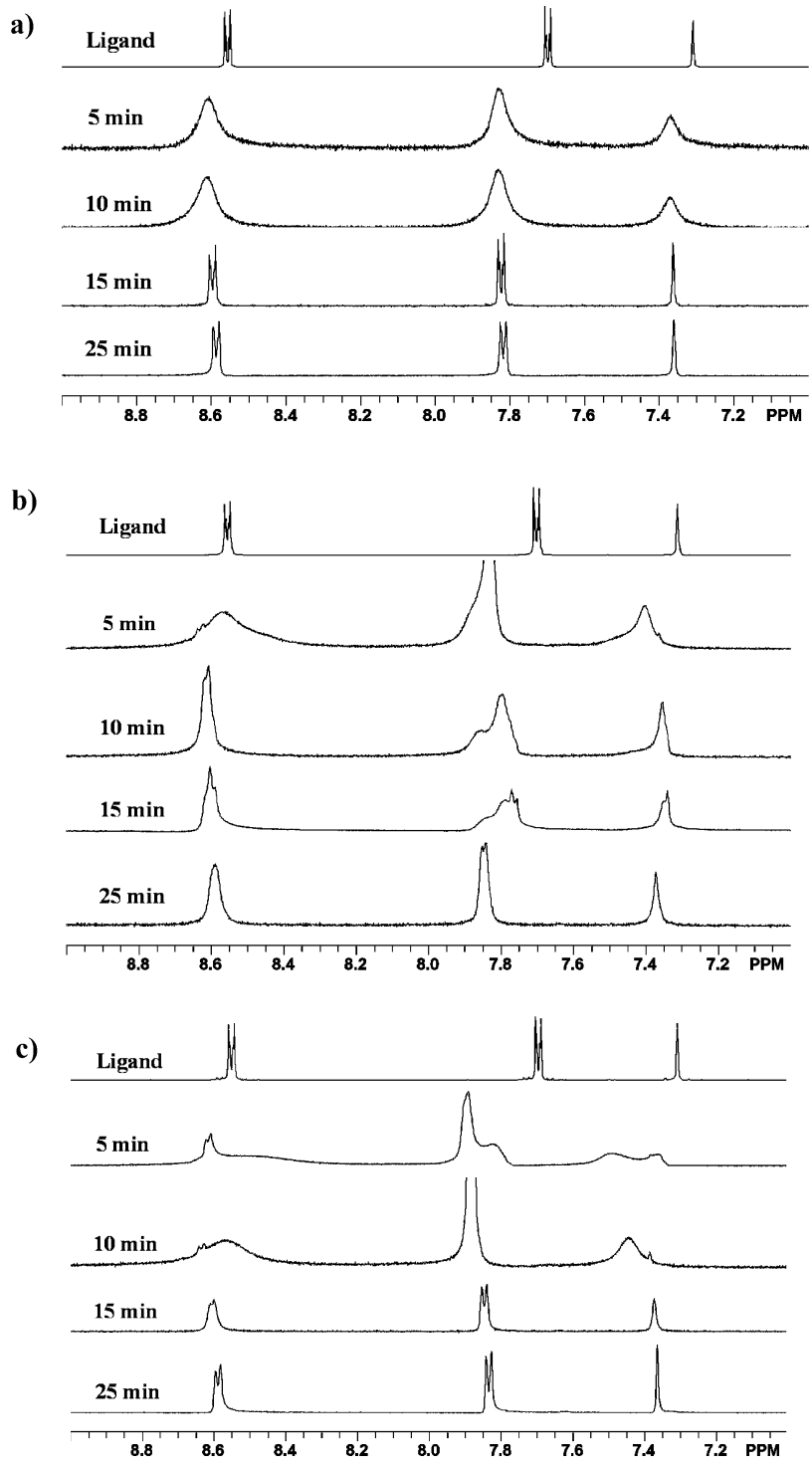

Figure 1. ^{1}H NMR spectra showing the self-assembly processes of **1** (a), **2** (b) and **3** (c).

value at 6 min, then narrow slightly and stabilize after equilibration for about 20−25 min. Overall, the resonances became significantly broadened and shifted downfield with respect to the free ligand (Figure 1), indicating that the coordination polymerization has occurred.

More information on the aggregation behavior of silver(I) salts and **L** in solution was obtained by absorption and CD spectroscopies. The coordination reaction of **L** with Ag(I) ion was monitored through a UV−vis spectroscopic titration. This experiment clearly showed that the coordination reaches the end point at a 1:1 ratio of Ag(I):**L**, as shown in parts a−c of Figure 2. This result indicates that a $(AgL)_n$ coordination polymer is produced. Results from the spectrophotometric titrations were corroborated by titrations followed by CD spectra. As depicted in parts d−f of Figure 2, clear spectral changes are observed upon the addition of Ag(I) aliquots to solutions of the (*S*)-**L** enantiomer. The CD signals come to plateau once a 1:1 molar ratio of Ag(I):**L** has been reached, as was the case for the spectrophotometric titration. Therefore, both UV−vis and CD spectra studies showed the formation of 1:1 monomer-to-metal complexes in solution.

In addition, with respect to that of the free ligand, both CD and UV−vis spectra of the reaction solutions of (*S*)-**L** and

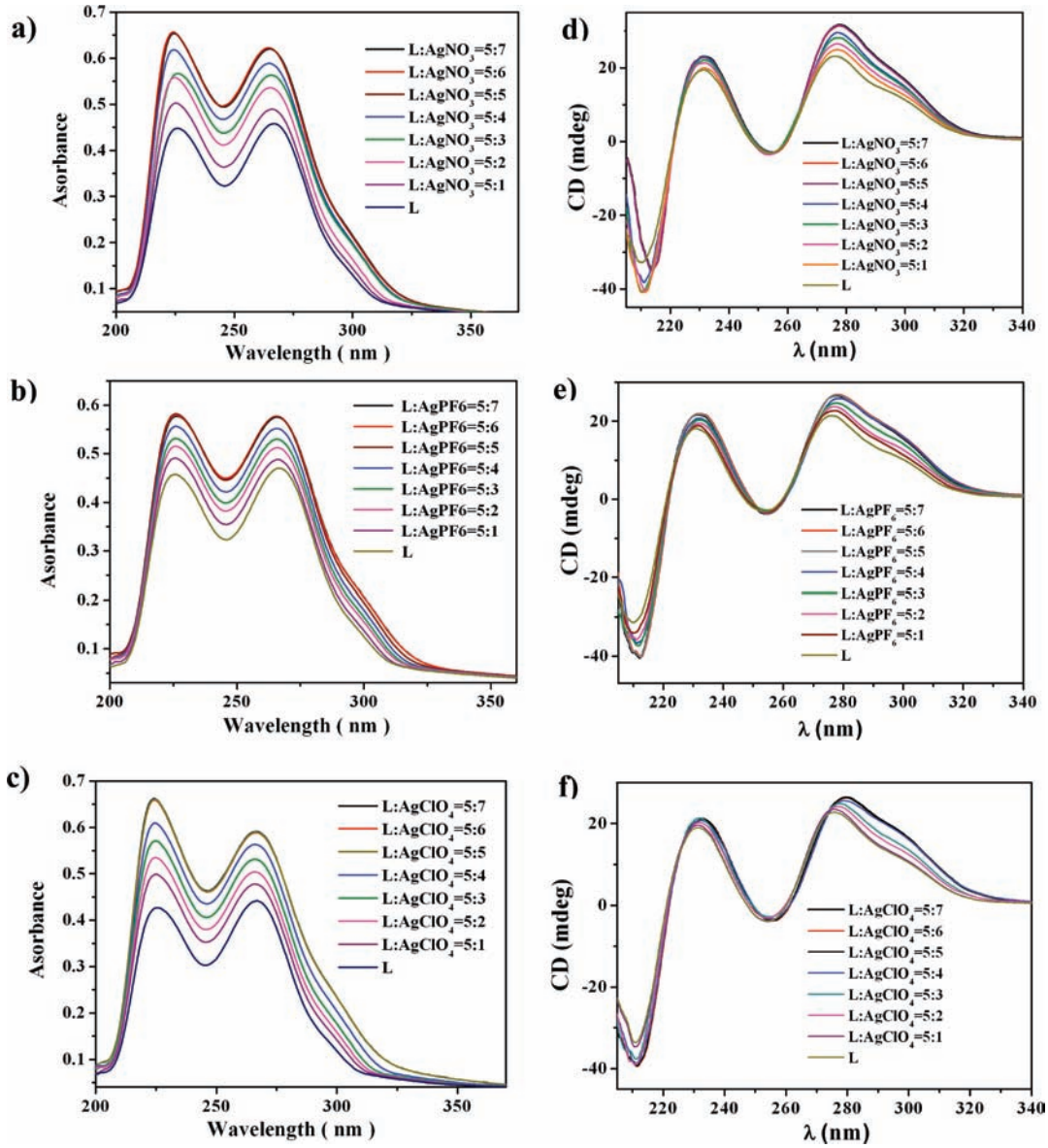

Figure 2. UV−vis and CD titrations of (*S*)-**L** (methanol) with AgX (methanol or H_2O): (a) and (d) for X = NO_3^-, (b) and (e) for X = PF_6^-, (c) and (f) for X = ClO_4^-.

Ag(I)X (X = NO_3^-, ClO_4^- or PF_6^-) showed obviously increase signals over the absorption ranges with the passage of time, which got stable after 20−25 min, indicative of the formation of a helical structure with a preferred handedness.

Having demonstrated from a combination of ^{1}H NMR, UV, and CD studies the formation of 1:1 monomer-to-metal complexes in solution, the next step was to investigate whether evidence could be obtained for the presence of coodination polymers in solution. Initial attempts to study the degree of polymerization by GPC using MeOH or THF as eluents were unsuccessful, due to the poor solubility of coordination polymers. The DMF solutions of **2** and **3** showed two apparent peaks with M_n = 5052 and M_w/M_n = 1.01 for **2** and M_n = 1807 and M_w/M_n = 1.50 for **3**, respectively, in the GPC profile by using polystyrene standards to give a rough estimate. Again, complex **1** exhibits poor solubility and thus it was not possible to obtain its molecular weight from DMF. Attempts were made to determine the molecular weight with MALDI-TOF spectra in MeOH, however, the results showed that three polymers all undergo severe fragmentation under those conditions. In all cases, the predominated fragments were detected at *m*/*z* 957.6, corresponding to $[Ag\mathbf{L}_2]^+$ species (Figures S25−27 in the Supporting Information).

Structure Description. [(AgL)NO_3] (1). A single-crystal X-ray diffraction study of complex ***M*-1** reveals a 3D chiral framework assembled from sextuple 2_1 helices constructed through argentophilic interactions. Complex ***M*-1** crystallizes in the chiral tetragonal space group $P4_12_12$, with three $AgNO_3$ units and three **L** ligands, three *i*-propanol and eight water guest molecules in the asymmetric unit. Three independent Ag centers each coordinates to two pyridyl groups of two different **L** in *trans* fashion with N−Ag−N angles of 165.5(15), 168.8(14) and 169.2(10) Å and the Ag−N bond lengths ranging from 2.112(4) to 2.156(4) Å (Figure 3). Adjacent metal centers are thus bridged by biphenyl backbones of **L** groups to form three independent infinite left-handed (***M***) helices, two of which run along the *b*-axis and one runs along the *c*-axis. All three such helices are generated around the crystallographic 2_1 axis with helical pitchs of 24.4911(18) and 28.7749(13) Å. The phenyl rings of the **L** ligands are twisted along the pivotal 1,1′-bond with dihedral

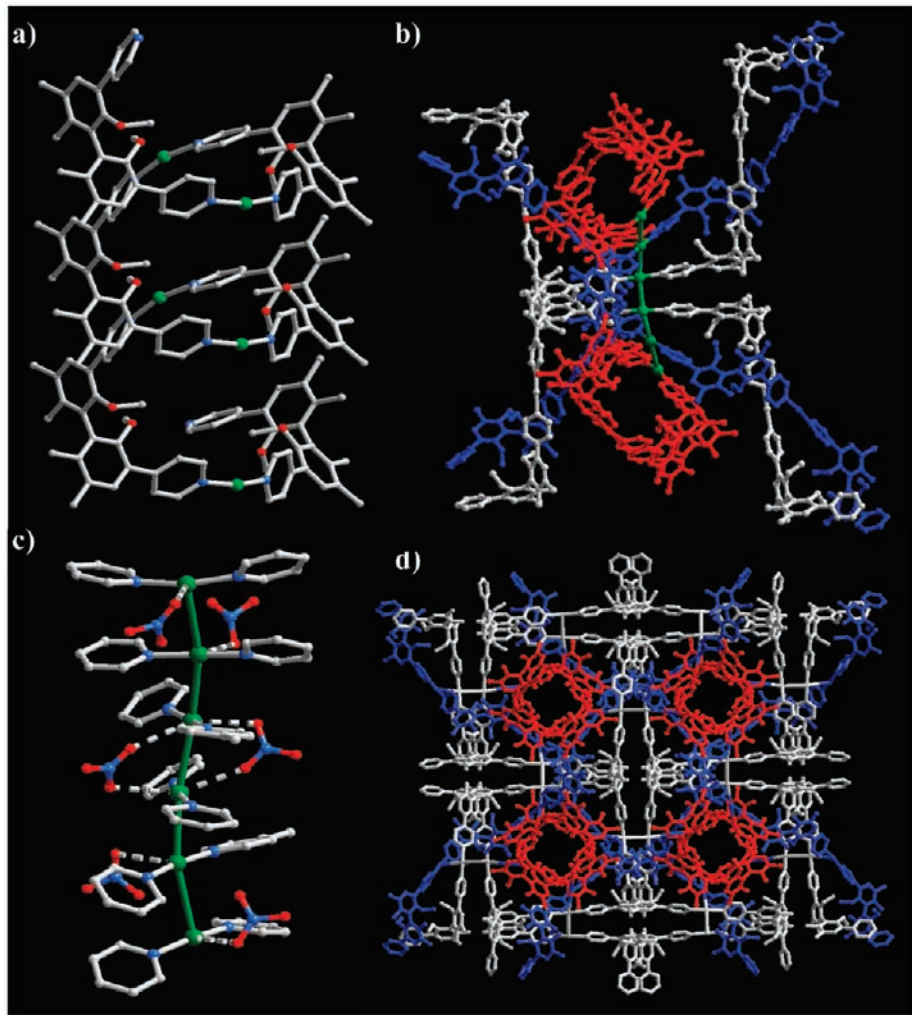

Figure 3. (a) One left-handed 2_1 helical chain in **1** built from alternating Ag(I) and **L**. (b) Six helical chains linked by argentophilic Ag−Ag interactions forming a sextuple helix. (c) A hexasilver(I) nanaowire surrounding by four monoadentate and two bidentate NO_3^- anions. (d) The 3D chiral framework of **1**.

angles of 80.21(12), 85.04(13) and 84.85(13)°; the bulk of the phenol moieties are pointing outward the helical axis and are thus well positioned to intertwine with other helices.

Three pairs of C_2-symmetry related helical strands shown in Figure 3 are interlinked by argentophilic Ag−Ag interactions to form a sextuply helix (Figure 3b and c). In the resulting Ag_6 chain, the two central silver atoms are bridged by two bidentate nitrate anions with a Ag−Ag distance of 3.3689(12) Å. While other four silver atoms, each linking to one nitrate oxygen atom, are involved in ligand unsupported argentophilic interactions with Ag−Ag distances of 3.2109(12) and 3.4878(14) Å, which are close to the van der Waals contact distance (3.44 Å). The Ag···O interacts are 2.757(10) and 2.838(9) Å for bidentate nitrates, 2.798(14) and 2.822(17) Å for monodentate nitrates. The Ag−Ag−Ag angles range from 166.834(37)° to 170.799(36)°, and the bent metallic axes lead to a zigzag silver nanowire with a length of 16.5229(17) Å. In addition, two helical strands involving terminal Ag atoms from different sextuple helices also intertwine each other *via* van der Waals interactions to form a double helix. Thus, such hexasilver(I) nanowires direct the packing of sextuple helices into a 3D chiral framework. Coordination-driven assembly of metallic nanowires into polymeric networks is unprecedented and holds great potential for making nanoscale hybrid materials by a bottom-up approach.[13] PLATON calculations indicate that complex **1** contains 35.4% void space (7763.0 Å^3 per unit cell) that is accessible to anions and solvent molecules.[14]

$[AgL(PF_6)_{1/6}(OH)_{5/6}]$ (2). Complex ***M*-2** adopts a chiral tubular framework assembled from interlinked nanotubes that are constructed from 3_1 double helices. ***M*-2** crystallizes in the chiral trigonal space group *R*32, with one $[Ag(PF_6)_{1/6}(OH)_{5/6}]$ unit, one **L** ligand and 3/2 MeOH, one CH_3CN and 3/2 H_2O guest molecules in the asymmetric unit. The Ag center coordinates to two pyridyl groups of two different **L** in *trans* fashion with an N−Ag−N angle of 167.88(18)° and Ag−N bond lengths of 2.181(4) and 2.184(4) Å (Figure 4). Adjacent silver centers are thus bridged by **L** ligands along the *c*-axis to form an infinite left-handed (***M***) helix, which is generated by a 3_1 axis with a pitch of 39.4914(11) Å. The phenyl rings of **L** have dihedral angles of 82.70(16), 82.67(20) and 82.58(21)°. The bulk of the

(13) Samuelson, L. *Mater. Today* **2003**, *6*, 22–31.
(14) Spek, A. L. *J. Appl. Crystallogr.* **2003**, *36*, 7–13.
(15) (a) Rais, D.; Yau, J.; Mingos, D. M. P.; Vilar, R.; White, A. J. P.; Williams, D. J. *Angew. Chem., Int. Ed.* **2001**, *40*, 3464–3467. (b) van der Velden, J. W. A.; Beurskens, P. T.; Bour, J. J.; Bosman, W. P.; Noordik, J. H.; Kolenbrander, M.; Buskes, J. A. K. M. *Inorg. Chem.* **1984**, *23*, 146.

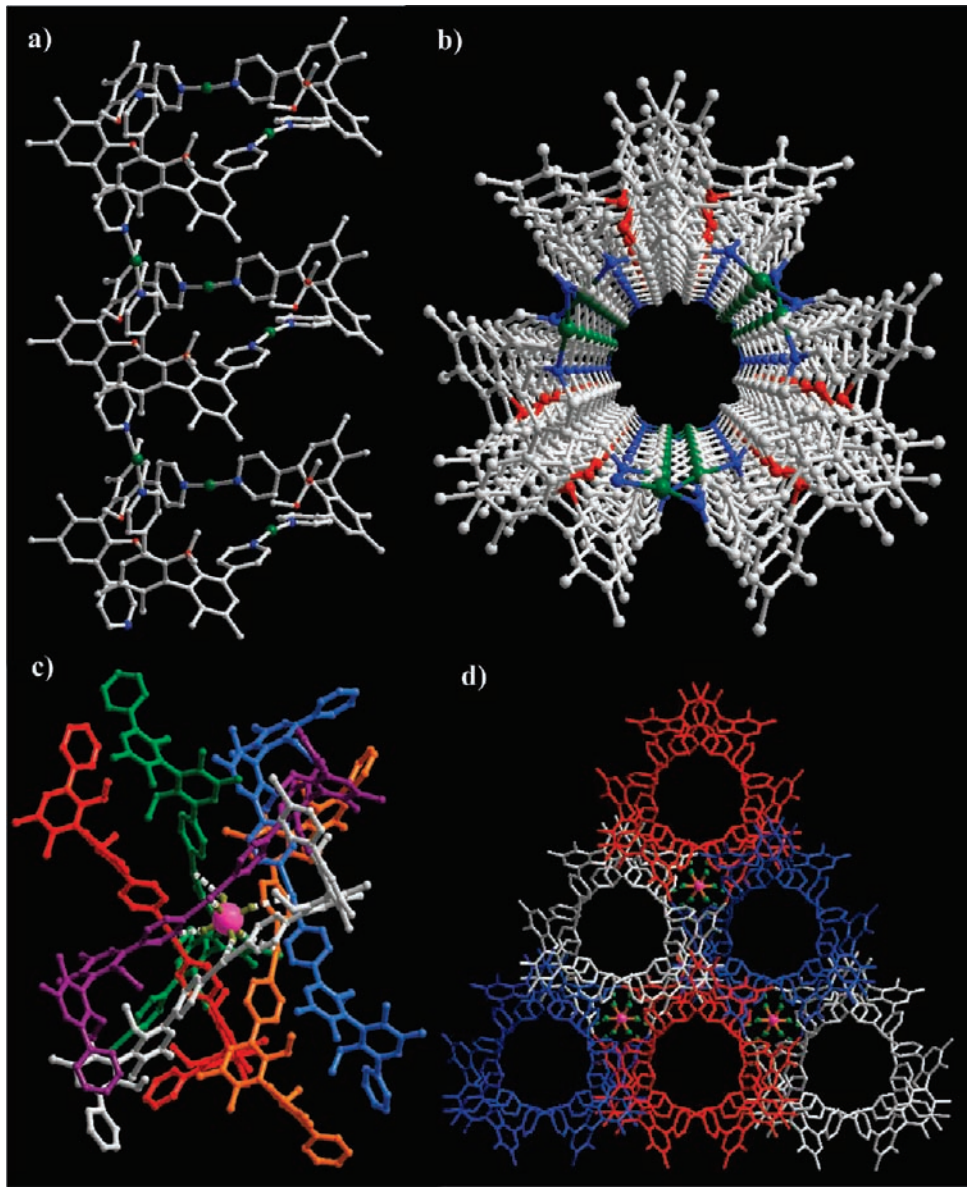

Figure 4. (a) One left-handed 3_1 helical chain in **2** built from alternating Ag(I) and **L**. (b) Parallel association of two helices into a chiral nanotube. (c) six helical chains templated by a PF_6^- anion forming a sextuple helix. (d) The 3D chiral framework of **2**.

phenyl moieties are pointing outward from the helical axis to generate a hollow cylinder.

Two infinite helical chains associate in parallel to form the wall of a trigonal tube with an opening of ~0.5 nm × 0.5 nm. Each double helix thus formed further associates with three other double helices from three different nanotubes around PF_6^- anions by forming weakly Ag−F [2.7797(24) Å] interactions to give a sextuply intertwined helix (Figure 4c). Therefore, the PF_6^- ions, each weakly binding to six 3_1 helices, direct packing of tubules in parallel to a 3D periodically ordered architecture with the slightly eclipsing of nanotube corners. Complex **2** contains 49.7% void space (9680.0 $Å^3$ per unit cell) that is accessible to counterions and solvent molecules.

[Ag(L)ClO$_4$] (3). Complex ***M*-3** adopts a chiral framework assembled from interlocking nanotubes that are constructed from double helices. ***M*-3** crystallizes in the chiral tetragonal space group $P4_322$, with one $AgClO_4$ unit, one **L** ligand and three water guest molecules in the asymmetric unit. The Ag center coordinates to two pyridyl groups of two different **L** in *trans* fashion with an N−Ag−N angle of 176.8(3)° and Ag−N bond lengths of 2.113(7) and 2.123(7) Å (Figure 5). Adjacent Ag centers are linked by **L** ligands along the *c*-axis to form an infinite left-handed (***M***) helix, which is generated around a 4_1 axis with a pitch of 24.1023(12) Å. The phenyl rings of **L** have a dihedral angle of 76.20(20)°. The bulk of the phenyl moieties are also pointing outward from the helical axis to generate a hollow cylinder.

Two infinite helical chains associate in parallel to form the wall of a tetragonal nanotube with an opening of ~1.7 nm × 1.7 nm. Each helix further intertwines with four other helices from four different nanotubes by forming weakly Ag−O [2.7369(12) Å] contacts with ClO_4^- anions, to give a periodically ordered interlocked architecture (Figure 5d). Therefore, the ClO_4^- anions, each weakly bridging two 4_1 helices, direct packing interlocked nanotubes in parallel to a 3D chiral framework with the significant eclipsing of nanotube corners. Severely eclipsed nanotubes have open channels of 3.1 Å ×

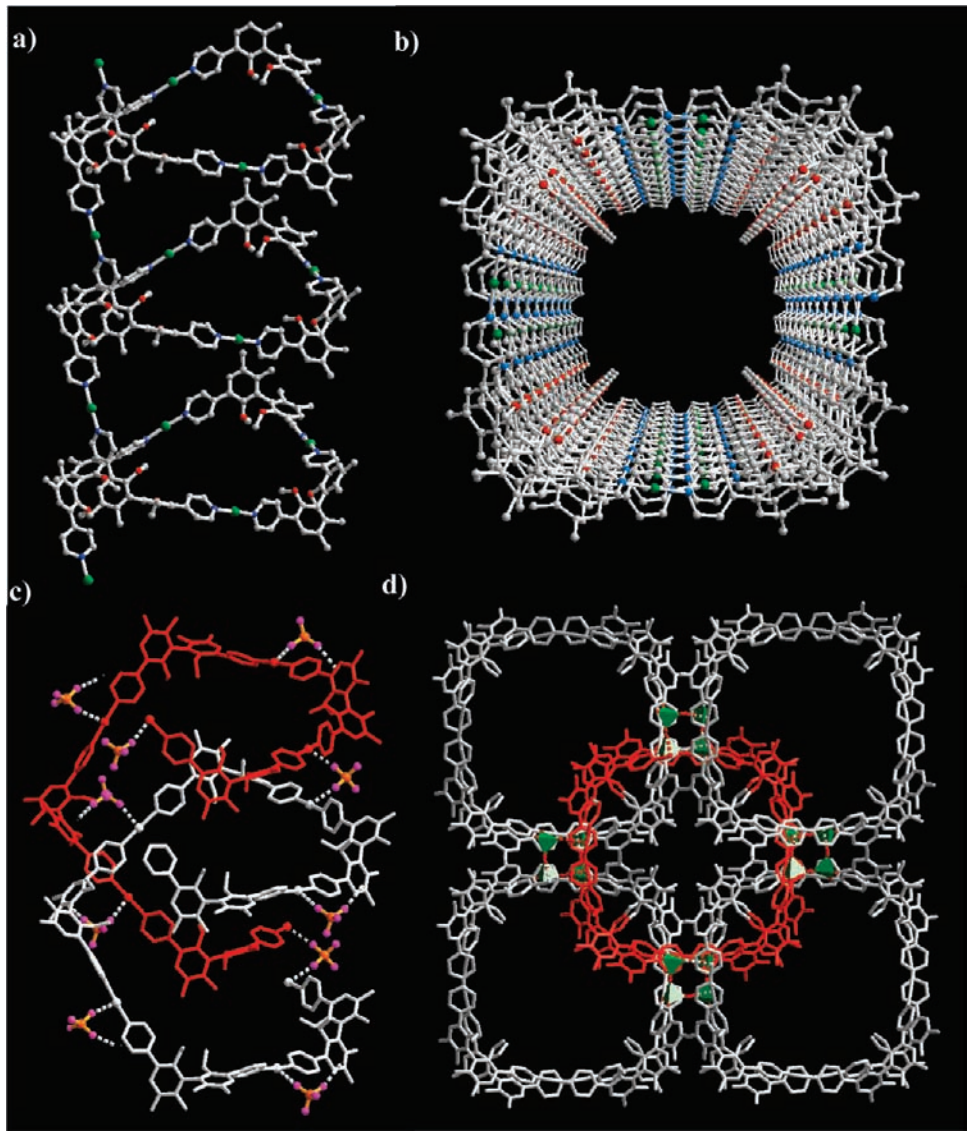

Figure 5. (a) One left-handed 4_1 helical chain in **3** built from alternating Ag(I) and **L**. (b) Parallel association of two helices into a chiral nanotube. (c) Two helical chains connected by bidentate ClO_4^- anions. (d) Interlocking of each nanotube with four other nanotubes. (The ClO_4^- anions are drawn as green tetrahedra.)

3.1 Å in dimensions. Complex **3** contains 42.1% void space (3091.7 $Å^3$ per unit cell) that is accessible to anions and solvent molecules.

Anion Effects on Helix Folding. The results described here demonstrate that, as the counteranions vary from NO_3^-, PF_6^- to ClO_4^-, the secondary structures of the coordination chains change from two-, three-, to four-fold helical conformations in the solid state. The basic skeleton of **1**−**3** is a cationic polymeric strand. Its formation is the result of a suitable combination of the skewed conformer of **L** and the linear geometry of the N−Ag−N bonds. Because each helical motif was constructed independent of the reaction stoichiometry, the solvents, and the concentrations of reactants, this variation can be attributed entirely to the difference in counteranions and may be rationalized by considering their sizes, geometries and binding abilities.

In the case nitrate as the counteranion, a cationic scaffold can effectively bind to the anion due to the relatively little steric repulsion. The ability to bind metal ions in diverse fashions allows nitrates to doubly bridge Ag(I) ions, generating a Ag−Ag bond in a bidentate mode. It promotes argentophilic interactions by giving a linear hexasilver(I) cluster that is stabilized by four monodentate nitrates. Although NO_3^- has a trigonal-planar symmetry, its small size excludes the possibility that anions template and organize polymeric chains into a C_3-symmetric structure for efficient binding. As a result, the polymeric strand folds into a two-fold helix.

Compared with NO_3^-, both PF_6^- and ClO_4^- are typical noncoordinating anions and have larger sizes and higher symmetries (tetrahedral and octahedral geometries, respectively). By using them as the counterions, as in compounds **2** and **3**, two helical structures in which the anions are not coordinated to the metal centers were achieved. As a result of the symmetry and steric demands, the ClO_4^- and PF_6^- ions are engaged in two and six sets of isolated weak Ag(I)−O and Ag(I)−F interactions, and act as templates to fold polymeric chains into three-fold and four-fold helices for **2** and **3**, respectively. An interesting feature of complex **2** is that only one in six of the anions is a PF_6^- binding to six helices, and the rest are hydroxide anions. Probably there is insufficient space for more octahedral anions to directly interact with helices, so the

compound crystallized more readily as a mixed OH^- and PF_6^- salt than as a pure PF_6^- salt. A similar situation was previously reported for high-symmetry metal clusters.[16]

A comparison of structures of **1**−**3** shows that this anion-driven self-assembly is accompanied by adaptive variations of the backbone conformations of **L** and the two-coordination geometries of Ag(I). From **1** to **3**, the average dihedral angles of **L** decrease from 83.4, 82.7 to 76.2°, while the N−Ag−N angles increase from 167.8, 167.9 to 176.8°.

The study of the folding of linear oligomers into well-defined conformations has received much attention.[4] For example, Moore and Wolynes have systematically studied helical folding of linear oligophenylacetylenes in solution.[5] The resulting structures are stabilized by noncovalent interactions such as solvophobic effect, hydrogen bonding, electrostatic, π,π-stacking interactions, and/or metal coordination. Moore reasoned that nonspecific secondary interactions provide the energetic driving force for folding, while directional interactions play a structure-defining role. Analogous folding behavior has been observed in the infinite polymers of complexes **1**−**3** in the solid state. Anion-directed assembly of both finite and infinite supramolecular structures has recently drawn much attention,[16] but helix folding has not been well studied.[8,17]The present result represents a significant example showing that variation of counteranions is a useful strategy to regulate the secondary structure of linear chain and thereby 3D supramolecular structure.

Solid State Properties. We have also prepared **1**−**3** using (*S*)-**L**. Solid-state CD spectra of **1**−**3** made from *R*- and *S*-enantiomers of **L** are mirror images of each other, indicating that the mutiple helices built from (*S*)-**L** is right-handed (***P***), and demonstrate their enantiomeric nature. Enantiopure bridging ligand **L** has thus steered the formation of homochiral helices of predictable handedness. While similar CD signals exhibited by **1**−**3** and **L**, suggesting their potential utility as chiroptical materials.

1−**3** exhibit intense photoluminescences in the solid state with the emission maximum at 381, 393, and 402 nm, respectively, upon excitation at 310 nm. These emission peaks are essentially the same as the solid-state fluorescence signal of free ligand **L** at 359 nm. We thus believed that the luminescence signals of **1**−**3** originate from ligand-centered n→π* or π→π* process.

Conclusion

We have demonstrated the self-assembly of three 3D homochiral frameworks based on periodically ordered arrays of helices built from a new C_2-symmetric bipyridyl-based biphenyl ligand and Ag(I) ions. The aggregation behavior of silver salts and **L** in solutions was investigated by a variety of techniques, including ^{1}H NMR, UV−vis, CD, GPC and MALDI-TOF. The conformation of the cationic helical chain exhibits remarkable dependence on the counteranions; NO_3^-, PF_6^- and ClO_4^- directed the polymeric strand to fold into 2_1, 3_1 and 4_1 helices, respectively. The 2_1 helices cross-link *via* argentophilic Ag−Ag interactions, forming sextuple helices which lead to a 3D chiral framework. Each pair of 3_1 or 4_1 helices associates in parallel to afford 3D tubular architectures. This unique self-assembly behavior could be explained by considering the sizes, geometries and binding abilities of the counteranions and subsequent chain conformation to minimize steric repulsions and maximize secondary interactions. The ability to control the helical conformations is a key to future synthesis of functional helical structures, which hold great promise in chiral technology and nanotechnology, and may also contribute to the understanding of helical organized systems in biology.[18]

Acknowledgment. This work was supported by the NSFC-20671062, "973" Program (2007CB209701 and 2009CB930403), NCET-05-0395 and the Shuguang Program (06SG12), the key project and the Scientific Research Foundation for the Returned Overseas Chinese Scholars of State Education Ministry.

Supporting Information Available: Additional spectroscopic data, structural plots and tables and full X-ray crystallographic information in CIF format. This material is available free of charge *via* the Internet at http://pubs.acs.org.

JA901154P

(16) (a) Beer, P. D.; Gale, P. A. *Angew.Chem., Int. Ed.* **2001**, *40*, 486–516. (b) Vilar, R. *Angew. Chem., Int. Ed.* **2003**, *42*, 1460–1477.

(17) (a) Jung, O.-S.; Kim, Y. J.; Lee, Y.-A.; Park, J. K.; Chae, H. K. *J. Am. Chem. Soc.* **2000**, *123*, 9921–9925. (b) Juwarker, H.; Lenhardt, J. M.; Pham, D. M.; Craig, S. L. *Angew. Chem., Int. Ed.* **2008**, *47*, 3740–3743. (c) Byrne, P.; Lloyd, G. O.; Anderson, K. M.; Clarke, N.; Steed, J. W. *Chem. Commun.* **2008**, 3720–3722.

(18) Heilman-Miller, S. L.; Thirumalai1, D.; Woodson, S. A. *J. Mol. Biol.* **2001**, *306*, 1157–1166.